Novel design proposed for nitride VCSELs

P. Mackowiak[1], R. P. Sarzala[1] and W. Nakwaski[1,2] (nakwaski@ck-sg.p.lodz.pl)
[1] Institute of Physics, Technical University of Lodz, ul. Wolczanska 219, Poland
[2] Center for High Technology Materials, University of New Mexico, Albuquerque, NM, USA

The InGaN/GaN quantum-well heterostructure has become the standard active medium in blue and violet nitride edge-emitting diode lasers that have just crossed the threshold of commercial availability. Their gain characteristics, however, suggest that also an operation of analogous nitride vertical-cavity surface-emitting lasers (VCSELs) could be possible [1]. There are recent reports [2,3] on optically-pumped nitride VCSELs. But it is still really difficult to achieve their efficient electrical pumping. Therefore the main goal of this work is to design a possible structure of nitride electrically-pumped VCSELs using the advanced simulation of their operation. Our model is based on the detailed effective-frequency optical approach [4] coupled with the finite-element current-spreading analysis.

At first we were analyzing the VCSEL geometry with intracavity contacts (an advanced double lateral injection design) which was proposed to avoid current penetration of nitride DBR mirrors [5]. For this design, the laser operation was found to be possible but its determined threshold currents were unacceptably high. This was due to a strong current crowding effect near the edges of the active region. Besides, the VCSEL resonator structure seems to be too thin to carry out the selective proton-implantation process, which in this design should leave unaffected upper and bottom layers of the current-spreading area.

Our further considerations were stimulated by the paper published by Song et al. [6]. They reported fabrication of the p-type contact in the form of annular rings, typically with 6 μm open aperture. This inspired us to propose a novel structure of an electrically-pumped nitride VCSEL with a diagonal current injection, shown in Fig. 1. Its layer thicknesses are listed in Table 1. Both contacts are assumed to have the same shape and sizes and are placed symmetrically with respect to the device axis. It is important to note, that in this case, the proton implantation used to form VCSEL high-resistivity areas does not need to be selective along the device axis; it may be performed across the whole VCSEL structure, which essentially facilitates this process.

For the fundamental radiation mode to be dominated, gain distributions within the circular VCSEL active region should be at least uniform, if not of a bell shape. It was found in the simulation that current injection close to uniform could be achieved when thicknesses of both the n-type and the p-type spacers were practically the same and additionally their resistivities were nearly equal. The latter is easy to be accomplished, using e.g. low Si ($2\cdot10^{17}$ cm^{-3}) doping of the n-spacer [7].

First results of our room-temperature (RT) simulation of the 10-μm VCSEL (r_A = 5 μm) are listed in Table 2. Calculated radial profiles of successive radiation radial modes are plotted in Fig. 2. As one can see, the profile of the fundamental LP_{01} mode is much better correlated with a uniform gain distribution than all other modes. Therefore the structure is found to be very selective (see Table 2): the fundamental mode distinctly exhibits the lowest threshold (line 1). Moreover the thresholds are steadily growing with an increase in the mode order (lines 2-8). It is a very beneficial result because, in most of VCSEL designs, higher-order modes are favoured due to a strongly nonuniform current-density distribution (see e.g. [5]). Besides RT threshold current densities are found to be very similar to those reported for arsenide and phosphide VCSELs, which is a direct consequence of low threshold gain values determined for the structure under consideration. It is important to note that the total voltage drop is dominated in more than 50% by the p-type contact. Extending dimensions of both contacts (lines 10-11) or placing them farther from the active region (line 9) practically does not affect the threshold condition, whereas it has a distinct impact on the total device voltage drop.

In conclusion, we have proposed a novel VCSEL design with a diagonal current injection for nitride diode lasers and demonstrated its very promising RT threshold characteristics.

Acknowledgement. The work was supported by the Polish State Committee for Scientific Research (KBN), grant No 8-T11B-025-17 and by the US-Poland M. Sklodowska-Curie Fund No MEN/NSF-98-336.

[1] P. Mackowiak and W. Nakwaski, *MRS Internet J. Nitride Semicond. Res*. **3** (1998) Article 35, *J. Phys. D: Appl. Phys*. **31** (1998) 2479 and **33** (2000) 642, *Opt. Quantum Electron.* **31** (1999) 1179.
[2] J.M. Redwing et al., *Appl. Phys. Lett*. **69** (1996) 1.
[3] Y.-K. Song et al., *Appl. Phys. Lett*. **76** (2000) 1662.
[4] H. Wenzel and H.-J. Wuensche, *IEEE J. Quantum Electron*. **33** (1997) 1156.
[5] G.A. Smolyakov et al., *Proc. SPIE* **3625** (1999) 324.
[6] Y.-K. Song et al., *Appl. Phys. Lett.* **74** (1999) 3720.
[7] W. Goetz et al., *Appl. Phys. Lett*. **68** (1996) 3144.

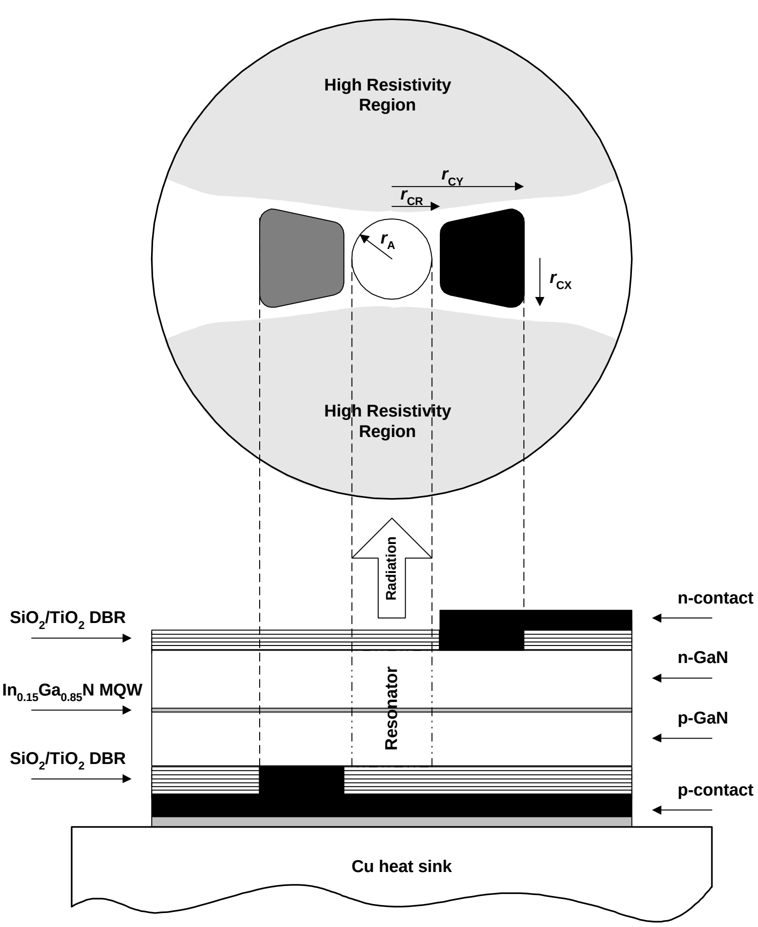

Fig.1. A scheme of a proposed electrically-pumped nitride VCSEL.

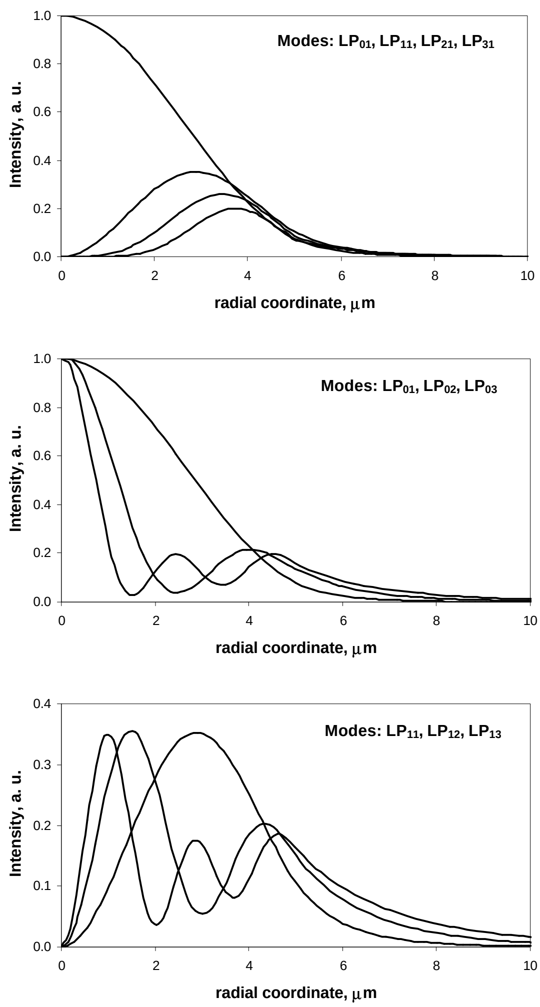

Fig. 2. Radial intensity profiles of LP modes.

layer	n_r	n_g	**d** nm	**α** cm^{-1}
SiO_2 (4) top DBR	1.56	1.61	64.1	10
TiO_2 (4) top DBR	3.00	5.00	33.3	10
n-GaN spacer	2.54	3.80	230	10
$In_{0.15}Ga_{0.85}N$ QW (5)	2.70	4.50	3.5	2000
$In_{0.02}Ga_{0.98}N$ barrier (4)	2.59	4.00	0.105	10
p-GaN spacer	2.54	3.80	228	10
SiO_2 (7) bottom DBR	1.56	1.61	64.1	10
TiO_2 (7) bottom DBR	3.00	5.00	33.3	10

Table 1. VCSEL parameters assumed in calculations; n_r - refractive index, n_g - group refractive index, d - layer thickness, a - absorption coefficient.

	Mode	$J_{p\text{-}n\ th}$ kA/cm^2	n_{th} $10^{19}cm^{-3}$	g_{th} cm^{-1}	I_{th} mA	U_{th} V	r_{CR} μm	r_{CX} μm	r_{CY} μm
1	**LP_{01}**	10.9	2.8	2027	13.9	21.4	5	5	15
2	**LP_{11}**	12.3	3.0	2447	15.6	23.6	5	5	15
3	**LP_{21}**	13.3	3.1	2759	17.0	25.4	5	5	15
4	**LP_{31}**	14.3	3.3	3053	18.3	27.1	5	5	15
5	**LP_{02}**	14.9	3.4	3220	19.0	28.1	5	5	15
6	**LP_{12}**	18.2	3.8	4089	23.3	33.7	5	5	15
7	**LP_{03}**	22.8	4.3	5168	29.1	41.3	5	5	15
8	**LP_{13}**	27.7	4.8	6206	35.2	49.5	5	5	15
9	**LP_{01}**	10.9	2.8	2027	27.8	39.6	10	5	15
10	**LP_{01}**	10.9	2.8	2027	13.9	13.7	5	10	15
11	**LP_{01}**	10.9	2.8	2027	13.9	21.4	5	5	25

Table 2. Results of the simulation for different LP modes; $J_{p\text{-}n}$ - current density at p-n junction, n - active region carrier density, g - material gain, I - device operating current, U - total device voltage drop, 'th' index indicates threshold values; r_{CX}, r_{CY}, r_{CR} describe contact size and position, see Fig.1